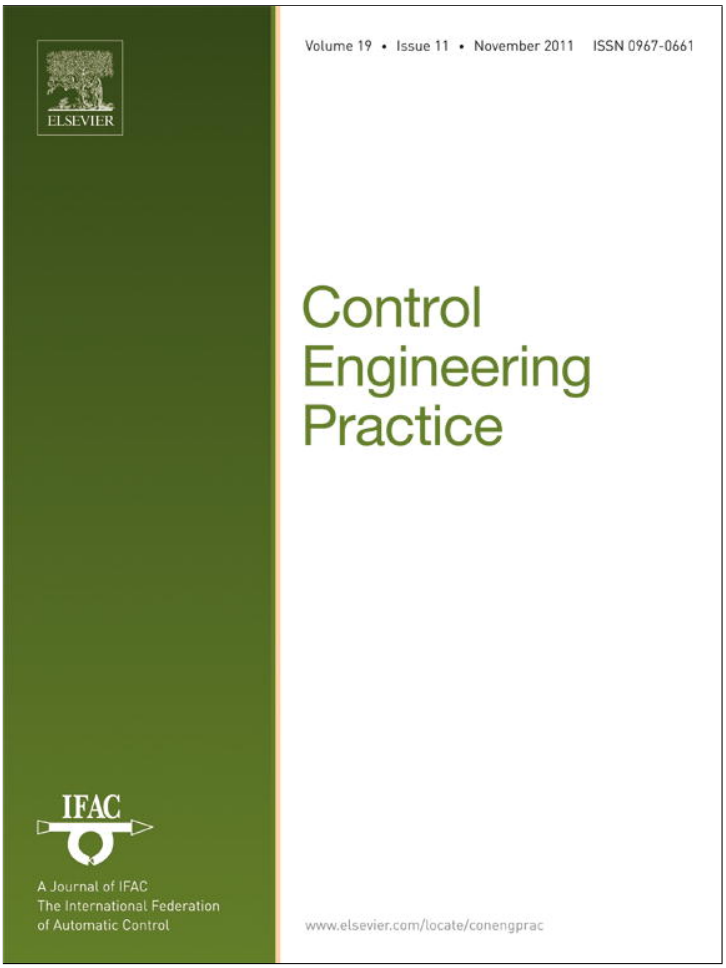

Control Engineering Practice 19 (2011) 1387–1397

Contents lists available at ScienceDirect

Control Engineering Practice

journal homepage: www.elsevier.com/locate/conengprac

Atomic-scale friction control by vibration using friction force microscope

Yi Guo [a,*], Zheng Wang [a], Zhihua Qu [b], Yehuda Braiman [c,d]

[a] Department of Electrical and Computer Engineering, Stevens Institute of Technology, Hoboken, NJ 07030, United States
[b] School of Electrical Engineering and Computer Science, University of Central Florida, Orlando, FL 32816, United States
[c] Center for Engineering Science Advanced Research, Computer Science and Mathematics Division, Oak Ridge National Laboratory, Oak Ridge, TN 37831, United States
[d] Department of Mechanical, Aerospace, and Biomedical Engineering, University of Tennessee Knoxville, Knoxville, TN 37996, United States

ARTICLE INFO

Article history:
Received 29 October 2010
Accepted 31 July 2011
Available online 23 August 2011

Keywords:
Nonlinear control
Friction
Vibration
Nano-scale systems
Friction force microscope

ABSTRACT

Manipulation of friction at the nanoscale has been traditionally approached by chemical means (lubrication). Recent friction force microscopy (FFM) experiments demonstrated that it can be done mechanically by applying vibration to accessible elements of the system. This paper provides analytic understanding on why vibration can reduce friction based on a 1D model imitating the FFM tip moving on a substrate. Open-loop stability is first studied, and a feedback vibration control is then designed using the accessible variable. Comparing to the open-loop system, friction force is significantly reduced in the closed-loop system. Numerical simulations show satisfactory performances.

1. Introduction

1.1. Friction control at the atomic-scale

Friction and wear is estimated to cost the US economy 6% of the gross national product (Persson, 2000). The study of nanoscale friction potentially has technological impacts in reducing energy loss in machines, in MEMS, and in the development of durable and low-friction surfaces and ultra thin lubrication films. Control of frictional properties, traditionally, is achieved by chemical means, supplementing base lubricants by so-called friction modifier additives, see Dudko, Filippov, Klafter, and Urbakh (2002) and the references therein. Recently, a different approach has attracted considerable interest, which is to control the system mechanically by applying small perturbations to accessible elements and parameters of the sliding system, see Braiman, Barhen, and Protopopescu (2003), Heuberger, Drummond, and Israelachvili (1998) and the references therein. The effect of small perturbations on frictional dynamics is a consequence of the highly nonlinear nature of the dynamic system (Urbakh, Klafter, Gourdon, & Israelachvili, 2004).

Using a surface force apparatus (SFA) modified to measure friction forces while inducing vibrations of one of the sliding surfaces, load- and frequency-dependent transitions between varieties of dynamical friction states can be observed which reveal regimes of extremely low friction (Heuberger et al., 1998). Friction properties are studied when one of the sliding surfaces is subjected to oscillations using an atomic force microscope (AFM) in Zaloj, Urbakh, and Klafter (1999), Tshiprut, Filippov, and Urbakh (2005), Socoliuc, Bennewitz, Gnecco, and Meyer (2004) and Socoliuc et al. (2006). As in the surface-force apparatus experiment (Heuberger et al., 1998), a significant reduction in the friction force and extremely low friction are observed. Recently, Jeon, Thundat, and Braiman (2006, 2007) employed a 1D frictional model to explain why vibration can reduce friction. In Jeon et al. (2007), numerical simulations are conducted on the effect of vibration parameters, and the results are compared with AFM experimental data. Despite successful experiments and recent simulation evidence, analytic understanding of the dynamic model and theoretical guidance on how to choose vibration parameters are missing (Guo, Qu, Braiman, Zhang, & Barhen, 2008). In this paper, the effect of in-plane vibration control on nanoscale friction is studied analytically using control theoretical methods.

1.2. Related work in vibration control

Vibrational control has been studied in controls community since the stabilization effect of an inverted pendulum by vibrating its support was observed and explained in Bogoliubov and Mitropolsky (1961). Initial work on developing a general theory of vibrational control was done in Meerkov (1980), which is followed by a series of work, for example, Bellman, Bentsman, and Meerkov (1986), Bentsman (1987), Shapiro and Zinn (1997), and Bullo (2002). Stabilizing effect of the dither signal, a high frequency signal introduced into a nonlinear system for the purpose of

* Corresponding author. Tel.: +1 201 216 5658; fax: +1 201 216 8246.
E-mail addresses: yi.guo@stevens.edu (Y. Guo), zheng.wang@stevens.edu (Z. Wang), qu@mail.ucf.edu (Z. Qu), braimany@ornl.gov (Y. Braiman).

0967-0661/$ - see front matter © 2011 Elsevier Ltd. All rights reserved.
doi:10.1016/j.conengprac.2011.07.014

augmenting stability or quenching undesirable jump-phenomena (Zames & Shneydor, 1977), was studied in macroscale systems with friction since the 1950s, see the recent paper (Pervozvanski & de Wit, 2002) and the references therein. However, friction dynamics in the macroscopic and microscopic systems have different properties, and friction control at the nanoscale poses new control challenges.

Frictional dynamics in macroscopic systems is adequately described by the motion of the center of mass since the effect of the atomistic motion on the motion of the center mass is insignificant relatively to the effect of all the applied forces. For microscopic size objects moving on the surface, the effect of the atomistic motion on center of mass dynamics may be significant and needs to be taken into consideration. This effect is in particular significant for microscopic size objects where the interparticle interaction of the atoms in a micro-cantilever is of the same order of magnitude as the interaction between the atoms of the cantilever with the atoms of the sliding surface. Therefore, our description of the motion of a micro-cantilever involves a set of coupled ordinary differential equations for each sliding atom on the surface, and the center of mass positions/velocities are calculated based on the positions/velocities of each individual particle. Consequently, it makes the control problem more complex and requires a different approach compared to control of a macroscopic object. Moreover, one can only apply control to the center of mass of the micro-cantilever, not to each individual particle. New experimental techniques, such as AFM and its modification known as friction force microscope (FFM), now allow well-defined experiments to be performed on well-characterized model system for the study of nanoscale friction (Klafter & Urbakh, 2007). In this paper, new feedback vibration control strategies are proposed to control friction based on an FFM model.

1.3. Contribution of the paper

In this paper, a dynamic model of the FFM system is first presented, which imitates the FFM tip as a 1D array of particles moving on a rigid substrate. Then, the open-loop stability is studied, which reveals that both the center of the mass and the individual particle systems are ultimately bounded under certain system parameters. However, the conditions are severe and the frictional force has approximately a non-zero constant magnitude. Due to the accessibility limitations of nanoscale systems, conventional feedback control is not feasible. A vibrational control scheme is designed, where high frequency vibration is applied to the substrate of the FFM sliding system in the lateral direction (parallel to the substrate). A tracking control problem is defined accordingly, and feedback vibration control is designed to tune the magnitude of vibration to stabilize the closed-loop tracking system thus to reduce friction. Through the process of direct separation of motion (Blekhman, 2000), where the high frequency oscillation is considered as a "fast" motion on the "slow" motion of the system, an approximation system is obtained for the "slow" dynamics with an effective potential due to the fast dynamics, and then the tracking control problem is solved. It is further proved that with relaxed conditions on system parameters, the individual particles in the tracking control system are asymptotically stable. Numerical simulations are conducted in Matlab, where the frictional forces are shown to be reduced to almost zero under vibration control.

The contribution of the paper is twofold. First, it advances analytic understanding of the FFM sliding model on surfaces and provides feedback vibration control scheme to guide the experimentalists choosing appropriate vibration parameters. Second, the system dynamics represents coupled nonlinear equations with constrained accessibility (*i.e.*, only the center of the mass position of the particle array is accessible for feedback). A new control method is developed to decouple the inter-connected system and to design feedback vibration control.

Note that throughout the paper, the friction force refers to the kinetic friction force.[1] The proposed model is based upon the best known among simple models in microscopic tribology, the Tomlinson model and the Frenkel–Kontorova model. However, the proposed model does not describe the comprehensive AFM structure and dynamics of that structure, but it is a tribological model that describes the dynamics of the sliding tip on the atomistic surfaces. (Interested readers are referred to Braun & Naumovets, 2006; Gnecco, Bennewitz, Gyalog, & Meyer, 2001; Vanossi & Braun, 2007 (among many other good survey papers) for more details on the atomic-scale friction models.)

The paper follows the same line of research as the authors' early publications (Guo & Qu, 2008; Guo et al., 2008) dealing with friction control at the nanoscale. However, the models proposed in Guo et al. (2008) and Guo and Qu (2008) refer to the Quartz Crystal Microbalance experimental setup where external forces can be applied to the sliding particles. Accordingly, feedback control is designed as a function of the particle position and velocity therein. The model proposed in the current paper is based on FFM experimental setup, where external forces can only be added to the system by vibrating the sliding substrate in the lateral direction. Also, the control method used in Guo et al. (2008) and Guo and Qu (2008) is based on Lyapunov stability analysis, while the main control technique used in the current paper is based on direct separation of motion in vibrational mechanics.

1.4. Organization and notations

The rest of the paper is organized as follows. In Section 2, a dynamic model of FFM sliding system is introduced, and a vibration control problem is defined. Then, the stability of the open-loop system is studied in Section 3. In Section 4, feedback vibration control is designed to solve the control problem defined. Simulation results are shown in Section 5. Finally, brief concluding remarks are presented in Section 6.

Notations: $\|x\|$ denotes the Euclidean norm of vector x. x^T denotes the transpose of vector x. I_N denotes the identity matrix of dimension N. diag$\{A_i\}$ denotes a block diagonal matrix whose diagonal elements are A_i. $\otimes$ denotes the Kronecker product.

2. The model and problem statement

2.1. Dynamic model of FFM sliding system

The AFM consists of a micro-cantilever with a sharp tip that slides on a surface and probes the surface topography. Typically, cantilever material is silicon or silicon nitride and tip radius is very sharp. The cantilever can move in both lateral and vertical directions. As the cantilever tip approaches the surface, an interaction force causes the cantilever to deflect. Light from a laser source reflects off the cantilever's tip and the corresponding change in cantilever deflection is recorded by a photodetector sensor. AFM can be used as an FFM to measure friction force between the cantilever tip and the sample scanned (Jeon et al.,

[1] The so-called *kinetic* friction force is the force required to maintain the two surfaces in relative motion at a steady velocity, while the so-called *static* friction force is defined as the minimal threshold force needed to initiate relative motion. They are distinct and fundamental concepts in tribology.

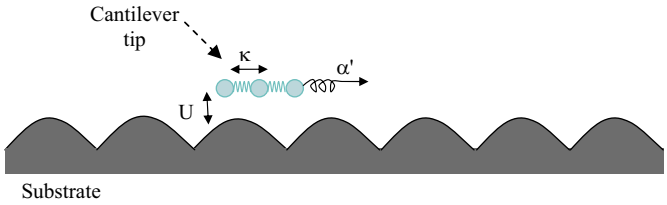

Fig. 1. A schematic illustration of the FFM model. The FFM tip is modeled as a particle chain, which is moving under a spring-like force.

2006; Ruan & Bhushan, 1994). When normal and lateral forces are measured at the same time, the AFM is called an FFM (Gnecco et al., 2001). Fig. 1 shows a schematic illustration of the FFM model.

In the model, we use a 1D Tomlinson/Frenkel Kontorova model of an array of N identical particles (atoms) moving on a periodic surface. The equations of motion of such a system can be written as the following:

$$m\ddot{\phi}_i+\gamma'\dot{\phi}_i+\frac{\partial U}{\partial \phi_i}=\alpha'(V_0't-\phi_{cm})+F_i(\phi_i,\phi_j), \tag{1}$$

where $i=1,\ldots,N$, ϕ_i is the coordinate of the ith particle, m is its mass, γ' is the linear friction coefficient representing the single particle energy exchange with the substrate, V_0' is the support velocity, and α' is the elastic spring constant of the FFM cantilever longitudinal mode. The particles in the array are subjected to a periodic potential, $U(\phi_i+a)=U(\phi_i)$ (where a is the lattice constant), and interact with each other via a pair-wise force, $F_i(\phi_i,\phi_j), j=i\pm 1$. The position of the center of mass is defined as $\phi_{cm}=(1/N)\sum_{i=1}^{N}\phi_i$.

Remark 1. This set of Eqs. (1) was recently used to describe the AFM experiment where the sliding surface was subject to normal vibrations and ultralow friction was observed and accurately (qualitatively) predicted the experimental results (Jeon et al., 2006, 2007). Modeling atomistic friction at the nanoscale is a very challenging problem and a variety of approaches has been proposed (Braiman, Family, & Hentschel, 1997; Elmer, 1997; Helman, Baltensperger, & Holyst, 1994; Hinrichs, 1997; Krylov & Frenken, 2009; Persson, 1997; Persson & Nitzan, 1996; Smith, Robbins, & Cieplak, 1996; Sokoloff, 1995; Weiss & Elmer, 1996; Zworner, Holscher, Schswarz, & Wiesendanger, 1998). In our approach, we consider the motion of a 1D chain of particles (atoms) moving on a periodic potential. The basic equation for the driven dynamics of such an array can be written in the following form:

$$m\ddot{\phi}_i+\gamma'\dot{\phi}_i+\frac{\partial U}{\partial \phi_i}=\alpha'(V_0't-\phi_{cm})+F_i(\phi_i,\phi_j)+\eta(t), \tag{2}$$

Here $\eta(t)$ is the Gaussian noise and $\langle\eta(t)\eta(t')\rangle=k_BT\gamma\delta(t-t')$. Eq. (2) for an array of particles follows from the widely used approach to describe the diffusion of a single atom on the surface in which case the equation of motion is given by: $m\ddot{\phi}+\gamma'\dot{\phi}+\partial U/\partial\phi=\eta(t)$ (Braun & Ferrando, 2002). In some cases, a nonlocal approach is used and the equation of motion reads as: $m\ddot{\phi}+\int_0^t\gamma(t-t')\ \dot{\phi}(t')\,dt'+\partial U/\partial\phi=\eta(t)$ (Miret-Artés & Pollak, 2005). In our approach, we combine many particles in a 1D array thus describing an array of coupled Langevin equations as in the reference Braun and Ferrando (2002), and we consider a limit of very low temperature thus the Gaussian noise term is not included in the equations. For the higher temperature case, we believe that since the proposed control design is robust, some level of noise will not affect it (however this issue needs to be looked in more detail).

A more detailed and possibly more realistic approach in modeling the dynamics of the AFM tip was proposed in the recent works (Abel, Krylov, & Frenken, 2007; Krylov & Frenken, 2008, 2009) where the dynamics of the AFM tip was described by the following equation: $m\ddot{\phi}_i+\gamma'\dot{\phi}_i+k(\phi-\phi_i(\phi))=\alpha'(V_0't-\phi_{cm})+\eta(t)$, where ϕ is the coordinate of the tip apex. A single-particle Langevin equation to describe the motion of the AFM tip was also used by Nakamura, Wakunami, and Natori (2005), however the motion of the apex was not included in their description.

2.2. Simplified model

We further assume the substrate potential to take a simple periodic form, and the same friction force acts on every atom, and we are interested in the time average of the friction force. To simplify the model (1), the structure lattice of the atoms of both the substrate and the tip are assumed to be equal.

Using the dimensionless variable $z_i=(2\pi\phi_i/a)$, where a is the surface periodicity parameter, after normalization (see Appendix A), the equation of motion (1) reduces to the following dimensionless form:

$$\ddot{z}_i+\gamma\dot{z}_i+\sin(z_i)=\alpha(V_0t-z_{cm})+F_i(z_i,z_j), \tag{3}$$

where z_{cm} is the position variable of the center of mass, that is,

$$z_{cm}=\frac{1}{N}\sum_{i=1}^{N}z_i. \tag{4}$$

The inter-particle force is assumed to be in the following form:

$$F_i(z_i,z_j)=\kappa(z_{i+1}-2z_i+z_{i-1}),\quad i=2,\ldots,N-1, \tag{5}$$

with the free-end boundary conditions:

$$F_1(z_1,z_2)=\kappa(z_2-z_1),$$

$$F_N(z_N,z_{N-1})=\kappa(z_{N-1}-z_N), \tag{6}$$

where κ is a positive constant.

Friction force is defined to be the difference between the external driving force αV_0t and the elastic spring force αz_{cm} (Helman et al., 1994) since the driving velocity is constant and the sum of all forces acting on the cantilever must be zero. We are interested in the time average of the friction force, and the friction force of the sliding system (3) is defined as

$$F_{fric}(t)=\frac{1}{t}\int_0^t\alpha(V_0\tau-z_{cm}(\tau))\,d\tau. \tag{7}$$

The objective of the paper is to study the stability property of the model (3), and to design vibrational control to reduce the friction force defined in (7). We define our control problem in the next subsection.

2.3. Control problem statement

Due to limited accessibility of the FFM system, conventional feedback control is not feasible. The effect of surface vibrations of friction was studied using FFM experiments in Jeon et al. (2006, 2007), where the procedure of the experiment and how friction is measured were explicitly presented. Numerical simulations of equations of motion (in dimensionless form) for a 1D array of atoms moving with a constant velocity on a rigid substrate were also performed in Jeon et al. (2006, 2007). Time-averaged friction force as a function of the vibration amplitude for a given vibration frequency are demonstrated therein. Good qualitative agreement with the experimental results are shown. It is shown that the friction force does not significantly depend on vibrations for small vibration frequencies and amplitude and drops significantly when the amplitude of vibration grows. For very large vibration frequencies friction force increases and reaches approximately

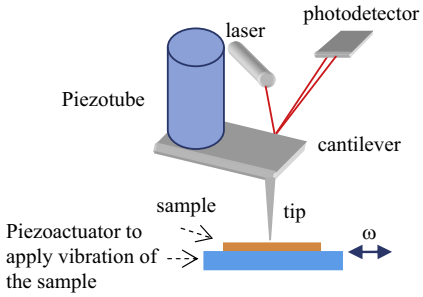

Fig. 2. Adding lateral vibration control to the FFM sliding system.

constant value that is independent on the vibration frequency. As the frequency range for friction reduction is significant, it is believed that the observed reduction is not a resonant effect and manifests significant change in friction dynamics due to vibrations.

Consider applying lateral (parallel to the surface) vibration to the substrate, which causes a time-periodic force acting on the particles, see Fig. 2. The equation of motion becomes (Klafter & Urbakh, 2007):

$$\ddot{z}_i+\gamma\dot{z}_i+\sin(z_i)=\alpha(V_0t-z_{cm})+F_i(z_i,z_j)+f_{vi}, \tag{8}$$

where f_{vi} is the vibration force acting on the particles.

It is concerned whether adding vibration can reduce friction force and how to choose vibration parameters accordingly. We propose a feedback scheme to control the external vibrational force amplitude so that the friction force defined in (7) is reduced. Since single particles are very difficult to access if at all possible, we only use the average quantity for feedback. We have the following assumption:

Assumption 1. The position of center of the mass of the particle array is measurable, that is, z_{cm} defined in (4) is available real time.

Note that the mass center position cannot be directly measured real time on the commercially available AFM platforms. However, with advanced control techniques (Miyoshi, Masuia, & Terashimaa, 2007; Rifai & Youcef-Toumia, 2007), precision positioning of the probe relative to the sample in all x–y–z-axes directions can be computed real time and used in feedback control, as shown in the literature including Wu and Zou (2009).

The main control problem is defined as follows:

Tracking Control Problem: Under Assumption 1, design vibration force f_{vi} in the following form:

$$f_{vi}=A(z_{cm},\omega,t)\sin(\omega t), \tag{9}$$

where $A(\cdot)$ is the feedback vibration magnitude to be designed, and ω is a constant (high) vibration frequency, such that the position of the center of the mass, z_{cm}, tracks the reference position signal V_0t in the system (8).

From the definition of the friction force (7), it can be seen that the friction force is proportional to the time integral of the tracking error $(z_{cm}-V_0t)$. Thus, solving the above defined tracking control problem will make the tracking error small so that the friction force is reduced. In the next section, we present the stability property of the open-loop system (3), which is followed by Section 4 on vibration control design to solve the tracking control problem defined above.

3. Open-loop stability

In this section, the stability property of the system (3) is studied. We first present a state-space model, and conduct local stability analysis using Lyapunov stability based methods. We reveal that under certain conditions on system parameters, the system (3) is locally ultimately bounded around the equilibrium points.

We first present state-space model of the system (3). Define state variables $x_{i1}=z_i$, and $x_{i2}=\dot{z}_i$, we have the following state-space representation:

$$\dot{x}_{i1}=x_{i2},$$

$$\dot{x}_{i2}=-\sin x_{i1}-\gamma x_{i2}+\alpha\left(V_0t-\frac{1}{N}\sum_{j=1}^{N}x_{j1}\right)+F_i(x_{i1},x_{j1}), \tag{10}$$

where $i=1,2\ldots,N$.

Assuming particle interaction as described in (5), and defining the error states as $e_{i1}=x_{i1}-V_0t, e_{i2}=x_{i2}-V_0$, we have

$$\dot{e}_{i1}=e_{i2},$$

$$\dot{e}_{i2}=-\sin(e_{i1}+V_0t)-\gamma(e_{i2}+V_0)-\frac{\alpha}{N}\sum_{j=1}^{N}e_{j1}+\kappa(e_{i+1,1}-2e_{i1}+e_{i-1,1}) \tag{11}$$

for $i=1,\ldots,N$. Note that with a little abuse of notation, the last term (on the particle interactions) in (11) becomes $\kappa(e_{21}-e_{11})$ for the first particle $i=1$, and $\kappa(e_{N-1,1}-e_{N1})$ for the last particle $i=N$, due to the free-end boundary condition defined in (6).

We define another state variable to remove the constant term in (11), $\xi_{i1}=e_{i1}+\gamma V_0/\alpha, \xi_{i2}=e_{i2}$. We have the following state-space model[2]:

$$\dot{\xi}_{i1}=\xi_{i2},$$

$$\dot{\xi}_{i2}=-\sin\left(\xi_{i1}+V_0t-\frac{\gamma V_0}{\alpha}\right)-\gamma\xi_{i2}-\frac{\alpha}{N}\sum_{j=1}^{N}\xi_{j1}+\kappa(\xi_{i+1,1}-2\xi_{i1}+\xi_{i-1,1}). \tag{12}$$

Eq. (12) represents an interconnected nonlinear system, which includes both a nearest-neighbor and an all-to-all particle interactions. We consider local stability of the system (12).

Linearizing the system around $(\xi_{i1}^*,\xi_{i2}^*)=(0,0)$, we obtain

$$\dot{\xi}_{i1}=\xi_{i2},$$

$$\dot{\xi}_{i2}=-\sin\left(V_0t-\frac{\gamma V_0}{\alpha}\right)-\cos\left(V_0t-\frac{\gamma V_0}{\alpha}\right)\xi_{i1}-\gamma\xi_{i2}-\frac{\alpha}{N}\sum_{j=1}^{N}\xi_{j1}+\kappa(\xi_{i+1,1}-2\xi_{i1}+\xi_{i-1,1}). \tag{13}$$

The above system represents an interconnected time-varying system. To facilitate stability analysis, we represent it in the following form:

$$\dot{\xi}=G\xi+f, \tag{14}$$

with

$$G=I_N\otimes\begin{bmatrix}0 & 1\\ -\cos\left(V_0t-\frac{\gamma V_0}{\alpha}\right) & -\gamma\end{bmatrix}+Q\otimes\begin{bmatrix}0 & 0\\ \kappa & 0\end{bmatrix}+J\otimes\begin{bmatrix}0 & 0\\ -\frac{\alpha}{N} & 0\end{bmatrix}, \tag{15}$$

$$f=\mathbf{1}\otimes\begin{bmatrix}0\\ -\sin\left(V_0t-\frac{\gamma V_0}{\alpha}\right)\end{bmatrix}, \tag{16}$$

[2] For the ease of presentation, we assume $\xi_{01}=\xi_{11}$ and $\xi_{N+1,1}=\xi_{N1}$ to account for the free-end boundary condition defined in (6).

where J is the N by N matrix of ones, $\mathbf{1}$ is the N-dimensional vector of ones, and

$$Q=\begin{bmatrix} -1 & 1 & 0 & \dots & 0 \\ 1 & -2 & 1 & 0 & \dots \\ & & \vdots & & \\ 0 & \dots & 1 & -2 & 1 \\ 0 & \dots & 0 & 1 & -1 \end{bmatrix}. \tag{17}$$

Because of the nearest-neighbor-connection structure as represented in Q, we can apply a similarity transformation to transform the linear part of the system (14) to a block diagonal one (Guo & Qu, 2008). Notice that the matrix $(-Q)$ is a real symmetric matrix with zero row sum, and it is irreducible. $(-Q)$ has eigenvalues:

$$\mu_1 \geq \mu_2 \geq \cdots \geq \mu_{N-1} > \mu_N = 0. \tag{18}$$

Denote the eigenvectors corresponding to each of the eigenvalues to be $v_k, k=1,2,\dots,N$. The trivial eigenvector of $(-Q)$, v_N, is uniform, and other non-trivial eigenvectors, $v_k, k=1,\dots,N-1$, are orthogonal to the trivial one. Let $V=[v_1\ v_2\ \dots\ v_N]$. We have $V^{-1}QV=-D_Q$ where D_Q is a diagonal matrix with the diagonal entry μ_i, $i=1,2,\dots,N$. The matrix V also transforms the all 1's matrix J into a diagonal one $V^{-1}JV=D_J$ where D_J is a diagonal matrix with diagonal entry $(D_J)_{ii}=0$, $i=1,2,\dots,N-1$, and $(D_J)_{NN}=N$.

Denote the transformation matrix as

$$T=V\otimes I_2. \tag{19}$$

We have

$$\begin{aligned} T^{-1}GT &= I_N\otimes\begin{bmatrix} 0 & 1 \\ -\cos\left(V_0t-\frac{\gamma V_0}{\alpha}\right) & -\gamma \end{bmatrix} \\ &\quad -D_Q\otimes\begin{bmatrix} 0 & 0 \\ \kappa & 0 \end{bmatrix}+D_J\otimes\begin{bmatrix} 0 & 0 \\ -\frac{\alpha}{N} & 0 \end{bmatrix} \\ &= \mathrm{diag}\{C_i\}, \end{aligned} \tag{20}$$

where

$$C_i=\begin{cases} \begin{bmatrix} 0 & 1 \\ -\cos\left(V_0t-\frac{\gamma V_0}{\alpha}\right)-\mu_i\kappa & -\gamma \end{bmatrix}, \\ \quad \text{for } i=1,2,\dots,N-1; \\ \begin{bmatrix} 0 & 1 \\ -\cos\left(V_0t-\frac{\gamma V_0}{\alpha}\right)-\alpha & -\gamma \end{bmatrix}, \\ \quad \text{for } i=N. \end{cases} \tag{21}$$

Now we have that the coupling of the system (14) is removed through a similarity transformation. We apply the state transformation, $\xi=T\phi$, to the complete system (14). We obtain the following system:

$$\dot{\phi}=\mathrm{diag}\{C_i\}\phi+\overline{f}, \tag{22}$$

where

$$\overline{f}=T^{-1}f=\begin{bmatrix} 0 \\ \vdots \\ 0 \\ \sqrt{N} \end{bmatrix}\otimes\begin{bmatrix} 0 \\ -\sin\left(V_0t-\frac{\gamma V_0}{\alpha}\right) \end{bmatrix}.$$

Due to the state transformation, the last subsystem in (22), ϕ_N, represents an average quantity, that is, $\phi_N=(1/\sqrt{N})\sum_{i=1}^{N}\xi_i$. We have

$$e_{cm1}\overset{def}{=}\frac{1}{N}\sum_{i=1}^{N}e_{i1}=\xi_{cm1}-\frac{\gamma V_0}{\alpha}=\frac{1}{\sqrt{N}}\phi_{N1}-\frac{\gamma V_0}{\alpha},$$

$$e_{cm2}\overset{def}{=}\frac{1}{N}\sum_{i=1}^{N}e_{i2}=\xi_{cm2}, \tag{23}$$

where $\xi_{cm1}\overset{def}{=}(1/N)\sum_{i=1}^{N}\xi_{i1}$, $\xi_{cm2}\overset{def}{=}(1/N)\sum_{i=1}^{N}\xi_{i2}$. Therefore, local stability of the average system can be analyzed using the ϕ_N subsystem.

3.1. Stability of the center of the mass

The dynamics of the ϕ_N subsystem is, according to (22),

$$\begin{aligned} \dot{\phi}_{N1} &= \phi_{N2}, \\ \dot{\phi}_{N2} &= \left[-\cos\left(V_0t-\frac{\gamma V_0}{\alpha}\right)-\alpha\right]\phi_{N1}-\gamma\phi_{N2}-\sqrt{N}\sin\left(V_0t-\frac{\gamma V_0}{\alpha}\right). \end{aligned} \tag{24}$$

Choose the Lyapunov function candidate,

$$W_N(t,\phi_N)=\left\{\frac{\varepsilon_N}{2}\phi_{N1}^2+\frac{1}{2}(\lambda_N\phi_{N1}+\phi_{N2})^2\right\}+\left\{\frac{1}{2}\left[1+\cos\left(V_0t-\frac{\gamma V_0}{\alpha}\right)\right]\phi_{N1}^2\right\}, \tag{25}$$

where ε_N and λ_N are positive design parameters. Taking the time derivative of W_N along the system trajectory (24), we can obtain the sufficient condition for the system (24) to be ultimately bounded, which is presented in the following proposition.

Proposition 1. *If the system parameter, α, satisfies the following condition*:

$$\alpha>\frac{V_0}{\gamma}+1, \tag{26}$$

the system (24) *is ultimately bounded.*

Proof. Considering the Lyapunov function candidate (25), its time derivative is

$$\begin{aligned} \dot{W}_N &= [\varepsilon_N+\lambda_N(\lambda_N-\gamma)-\alpha+1]\phi_{N1}\phi_{N2}+[-\lambda_n\cos(V_0t-\delta)-\alpha\lambda_N \\ &\quad -\tfrac{1}{2}V_0\sin(V_0t-\delta)]\phi_{N1}^2+(\lambda_N-\gamma)\phi_{N2}^2-\sqrt{N}(\lambda_N\phi_{N1}-\phi_{N2})\sin(V_0t-\delta), \end{aligned} \tag{27}$$

where we denote $\delta=\gamma V_0/\alpha$. If $\alpha>1$, we can choose the design parameter $\lambda_N=\gamma/2$, and $\varepsilon_N=\lambda_n(\gamma-\lambda_N)+\alpha-1$ to cancel out the cross-term. Bounding the sinusoidal terms, we obtain

$$\dot{W}_N\leq-[(\alpha-1)\lambda_N-\tfrac{1}{2}V_0]\phi_{N1}^2-(\gamma-\lambda_N)\phi_{N2}^2+\sqrt{N(\lambda_N^2+1)}\|\phi_N\|, \tag{28}$$

where $\|\phi_N\|$ denote the Euclidean norm of ϕ_N.

If $\alpha>V_0/\gamma+1$, let

$$(\alpha-1)\lambda_N-\tfrac{1}{2}V_0\overset{def}{=}a>0,\quad \gamma-\lambda_N\overset{def}{=}b>0, \tag{29}$$

and define

$$\theta<\min\{a,b\}. \tag{30}$$

We have

$$\dot{W}_N\leq-(a-\theta)\phi_{N1}^2-(b-\theta)\phi_{N2}^2-\theta\|\phi_N\|^2+\sqrt{N(\lambda_N^2+1)}\|\phi_N\|, \tag{31}$$

which implies

$$\dot{W}_N\leqslant-(a-\theta)\phi_{N1}^2-(b-\theta)\phi_{N2}^2,\quad \forall\|\phi_N\|\geq\frac{\sqrt{N(\lambda_N^2+1)}}{\theta}. \tag{32}$$

According to Theorem 4.18 in Khalil (2002), we conclude that the system (24) is ultimately bounded. □

3.2. Single particle stability

In addition to the conditions in (26), we need additional conditions to ensure each individual particle in the system (22) to be bounded. We have the following proposition.

Proposition 2. *If the system parameters, α, and κ, satisfy the following conditions*:

$$\alpha > \frac{V_0}{\gamma}+1, \quad \kappa > \frac{1}{\mu_{N-1}}+\frac{V_0}{\gamma\mu_{N-1}}, \tag{33}$$

where μ_{N-1} is the second smallest eigenvalue of $(-Q)$ as defined in (17), *the system* (22) *is ultimately bounded.*

Proof (*Sketch*). In addition to the stability of the Nth subsystem of (22) as presented in Proposition 1, we consider the stability of the subsystem $i, i=1,\ldots,N-1$. Choose the Lyapunov function candidate:

$$W=\sum_{i=1}^{N-1}\left\{\frac{\varepsilon_i}{2}\phi_{i1}^2+\frac{1}{2}(\lambda_i\phi_{i1}+z_{i2})^2\right\}+\sum_{i=1}^{N-1}\left\{\frac{1}{2}\left[1+\cos\left(V_0t-\frac{\gamma V_0}{\alpha}\right)\right]\phi_{i1}^2\right\}, \tag{34}$$

where ε_i and $\lambda_i, i=1,\ldots,N-1$, are design parameters. Following the same procedure as described in the proof of Proposition 1 and also the proof of Theorem 3 in Guo and Qu (2008), we obtain the additional condition on $\kappa: \kappa > 1/\mu_{N-1}+V_0/\gamma\mu_{N-1}$. Combining the above conditions with those in Proposition 1, we obtain (33). □

We summarize the main results in the following theorem on the open-loop stability.

Theorem 1 (*Open-loop stability*). *The center of the mass of the system* (13) *is locally ultimately bounded around its equilibrium point* $(\xi_{cm1},\xi_{cm2})=(0,0)$ *if the system parameter α satisfies the condition defined in* (26). *Furthermore, if the system parameters α,κ satisfy the condition defined in* (33), *each individual particle of the system* (13) *is locally ultimately bounded around the equilibrium point* $(\xi_{i1},\xi_{i2})=(0,0)$ *for* $i=1,\ldots,N$.

The theorem follows directly from Propositions 1 and 2.

Remark 2. Since the application of Lyapunov direct method provides sufficient conditions only, the obtained conditions on system parameters are sufficient and may be conservative.

From Theorem 1, we can see that the linearized system (13) is locally ultimately bounded around the equilibrium points under certain conditions on system parameters. It implies that the friction force, as defined in (7), is bounded around $\gamma V_0/\alpha$. We can also see that the condition on system parameters for ultimate boundedness of the single particle system is more severe than that for the center of the mass system. This is consistent with the physical intuition that extra effort is needed to stabilize individual particles, since each particle could be unstable even the center of the mass is stable.

In the next section, we design feedback vibration control and solve the control problem defined in Section 2.3.

4. Vibration control design

In this section, feedback vibrational control is designed using the technique of direct separation of motion in vibrational mechanics (Blekhman, 2000). Due to Assumption 1, we can only use the position variable of the center of the mass for feedback.

Consider the following vibration control:

$$f_{vi}=\sin(\omega t)\cdot\left(\omega\sqrt{2ke^2-4\gamma V_0e-4\sin(V_0t)e+c}\right), \tag{35}$$

where

$$e=z_{cm}-V_0t, \tag{36}$$

and k,c are positive control parameters and c is chosen to ensure the argument in the square root sign positive, that is, $c>(2/k)(\gamma V_0+1)^2$. Note that (35) is chosen through a reverse design of direct separation of motion (Blekhman, 2000) and Lyapunov design (Khalil, 2002; Qu, 1998). From the process presented below, we can see through a Lyapunov analysis that the feedback vibration control law (35) provides a desired closed-loop response of the approximate system.

Substituting (35) into (8), we obtain the closed-loop system as follows:

$$\ddot{z}_i+\gamma\dot{z}_i+\sin(z_i)=\alpha e+F_i(z_i,z_j)+\sin(\omega t)\cdot\left(\omega\sqrt{2ke^2-4\gamma V_0e-4\sin(V_0t)e+c}\right). \tag{37}$$

Re-write (37) into the following form as

$$\ddot{z}_i=W_i(\dot{z}_i,z_i,t)+\Phi_i(z_i,t,\tau),$$

$$W_i(\dot{z}_i,z_i,t)=-\gamma\dot{z}_i-\sin(z_i)+\alpha e+F_i(z_i,z_j),$$

$$\Phi_i(z_i,t,\tau)=\sin(\tau)\cdot\omega\cdot\sqrt{2ke^2-4\gamma V_0e-4\sin(V_0t)e+c}, \tag{38}$$

where $\tau=\omega t$, and

$$\int_0^T\Phi_i(z_i,t,\tau)\,d\tau=0 \quad \text{at fixed } z_i,t \tag{39}$$

with $T=2\pi/\omega$.

Consider its solution in the following form:

$$z_i=Z_i(t)+\Psi_i(t,\tau), \tag{40}$$

where Ψ_i satisfies

$$\int_0^T\Psi_i(t,\tau)\,d\tau=0. \tag{41}$$

Substituting (40) into (38) gives

$$\ddot{Z}_i+\ddot{\Psi}_i=W_i(\dot{Z}_i+\dot{\Psi}_i,Z_i+\Psi_i,t)-W_i(\dot{Z}_i,Z_i,t)+W_i(\dot{Z}_i,Z_i,t)+\Phi_i(Z_i+\Psi_i,t,\tau). \tag{42}$$

Averaging both sides of (42) with respect to the fast time τ and using (41) gives

$$\ddot{Z}_i=W_i(\dot{Z}_i,Z_i,t)+\frac{1}{T}\int_0^T[W_i(\dot{Z}_i+\dot{\Psi}_i,Z_i+\Psi_i,t)-W_i(\dot{Z}_i,Z_i,t)]\,d\tau+\frac{1}{T}\int_0^T\Phi_i(Z_i+\Psi_i,t,\tau)\,d\tau. \tag{43}$$

Subtracting (43) from (42) gives

$$\ddot{\Psi}_i=W_i(\dot{Z}_i+\dot{\Psi}_i,Z_i+\Psi_i,t)-W_i(\dot{Z}_i,Z_i,t)-\frac{1}{T}\int_0^T[W_i(\dot{Z}_i+\dot{\Psi}_i,Z_i+\Psi_i,t)-W_i(\dot{Z}_i,Z_i,t)]\,d\tau+\Phi_i(Z_i+\Psi_i,t,\tau)-\frac{1}{T}\int_0^T\Phi_i(Z_i+\Psi_i,t,\tau)\,d\tau. \tag{44}$$

To find a solution to (44), we resort to approximation methods. Note that W_i represents the slow motion component, which changes very little in one fast time period $T=2\pi/\omega$ comparing to the fast component Φ_i. We have

$$\left|\tilde{W}_i-\frac{1}{T}\int_0^T\tilde{W}_i\,d\tau\right|\ll\left|\Phi_i-\frac{1}{T}\int_0^T\Phi_i\,d\tau\right|, \tag{45}$$

where

$$\tilde{W}_i=W_i(\dot{Z}_i+\dot{\Psi}_i,Z_i+\Psi_i,t)-W_i(\dot{Z}_i,Z_i,t).$$

So the first three terms in (44) can be neglected. Also, according to (39),

$$\frac{1}{T}\int_0^T\Phi_i(Z_i+\Psi_i,t,\tau)\,d\tau=0 \tag{46}$$

at frozen Z_i,Ψ_i, and t.

Because of (45) and (46), (44) can be approximated by

$$\ddot{\Psi}_i = \Phi_i(Z_i+\Psi_i,t,\tau) = \omega \sin(\tau)\left(\sqrt{2ke^2-4\gamma V_0 e-4\sin(V_0t)e+c}\right), \tag{47}$$

whose solution at frozen e is

$$\Psi_i^* = -\varepsilon \sin(\omega t)\cdot\left(\sqrt{2ke^2-4\gamma V_0 e-4\sin(V_0t)e+c}\right), \tag{48}$$

where $\varepsilon = 1/\omega$. We can see that the magnitude of Ψ_i is of the order of $\varepsilon|Z_i|$, that is to say, the ratio of the two variables, Ψ_i/Z_i, is of the order of ε. Therefore, we can neglect the term Ψ_i in $W_i(\dot{Z}_i+\dot{\Psi}_i,Z_i+\Psi_i,t)$.

Since

$$\Phi_i(Z_i+\Psi_i,t,\tau)-\Phi_i(Z_i,t,\tau) \approx \frac{\partial \Phi_i(Z_i,t,\tau)}{\partial Z_i}\Psi_i, \tag{49}$$

we have

$$\begin{aligned}\frac{1}{T}\int_0^T \Phi_i(Z_i+\Psi_i,t,\tau)\,d\tau &= \frac{1}{T}\int_0^T \Phi_i(Z_i,t,\tau)\,d\tau + \frac{1}{T}\int_0^T \frac{\partial \Phi_i(Z_i,t,\tau)}{\partial Z_i}\Psi_i\,d\tau \\ &= \frac{1}{T}\int_0^T \frac{\partial \Phi_i(Z_i,t,\tau)}{\partial Z_i}\Psi_i\,d\tau.\end{aligned} \tag{50}$$

Note that the second equal sign holds due to (39).

Substituting (48) and (50) into (43), we obtain

$$\begin{aligned}\ddot{Z}_i = W_i(\dot{Z}_i,Z_i,t) &+ \frac{1}{T}\int_0^T [W(\dot{Z}_i+\dot{\Psi}_i^*,Z_i,t) \\ &- W(\dot{Z}_i,Z_i,t)]\,d\tau + \frac{1}{T}\int_0^T \frac{\partial \Phi_i(Z_i,t,\tau)}{\partial Z_i}\Psi_i^*\,d\tau.\end{aligned} \tag{51}$$

Therefore, we have the approximation system to (37):

$$\ddot{Z}_i+\gamma\dot{Z}_i+\sin(Z_i) = \alpha(V_0t-Z_{cm})+F_i(z_i,z_j)-kE+\gamma V_0+\sin(V_0t), \tag{52}$$

where Z_i is the state of the approximation system, $Z_{cm} = (1/N)\sum_{i=1}^N Z_i$, and $E = Z_{cm}-V_0t$.

Next, we analyze the stability of the approximation system (52), with the understanding that the error of the solutions between the original one (37) and this one is up to the order of $\varepsilon = 1/\omega$.

Denoting $E_{i1} = Z_i - V_0t, E_{i2} = \dot{Z}_i - V_0$, assuming linear inter-particle connection in the form of (5), we can represent (52) in the error space,

$$\begin{aligned}\dot{E}_{i1} &= E_{i2},\\ \dot{E}_{i2} &= -\frac{(\alpha+k)}{N}\sum_{j=1}^N E_{j1}-\gamma E_{i2}-\sin(E_{i1}+V_0t)+\sin(V_0t)\\ &\quad +\kappa(E_{i+1,1}-2E_{i1}+E_{i-1,1}).\end{aligned} \tag{53}$$

Adding up (53) for $i = 1,\ldots,N$, and denoting

$$E_{cm1} = E = \frac{1}{N}\sum_{i=1}^N E_{i1}, \tag{54}$$

$$E_{cm2} = \frac{1}{N}\sum_{i=1}^N E_{i2}, \tag{55}$$

we get the error dynamics of the center of the mass:

$$\begin{aligned}\dot{E}_{cm1} &= E_{cm2},\\ \dot{E}_{cm2} &= -(\alpha+k)E_{cm1}-\gamma E_{cm2}-\frac{1}{N}\sum_{i=1}^N \sin(E_{i1}+V_0t)+\sin(V_0t).\end{aligned} \tag{56}$$

Note that the last two terms of the second equation of (56) can be simplified using

$$\sin V_0t-\sin(E_{i1}+V_0t) = -2\sin\frac{E_{i1}}{2}\cos\frac{E_{i1}+2V_0t}{2}. \tag{57}$$

Next, we present stability results of the center of the mass system (56), which solve the Tracking Control Problem defined in Section 2.3.

4.1. Center of the mass system

It can be seen from (56) that the equilibrium of the center of the mass is $(E_{cm1},E_{cm2}) = (0,0)$. We choose the Lyapunov function candidate for (56) as

$$\begin{aligned}V(E_{cm1},E_{cm2}) &= \frac{a^2}{2}E_{cm1}^2+\frac{1}{2}E_{cm2}^2+bE_{cm1}E_{cm2}\\ &= \frac{1}{2}\left(aE_{cm1}+\frac{b}{a}E_{cm2}\right)^2+\frac{1}{2}\left(1-\frac{b^2}{a^2}\right)E_{cm2}^2,\end{aligned} \tag{58}$$

where $a = \sqrt{(k+\alpha)+\gamma^2/2}$ and $b = \gamma/2$. Since $b<a$, the Lyapunov function defined above is positive definite.

Taking the derivative of the Lyapunov function with respect to t along the solution of (56), we have

$$\begin{aligned}\dot{V} &= -\gamma E_{cm2}^2-b(k+\alpha)E_{cm1}^2-\frac{2(bE_{cm1}+E_{cm2})}{N}\\ &\quad\cdot\sum_{i=1}^N \cos\left(\frac{E_i+2V_0t}{2}\right)\sin\left(\frac{E_i}{2}\right)\\ &\le -\gamma E_{cm2}^2-b(k+\alpha)E_{cm1}^2+2(b|E_{cm1}|+|E_{cm2}|)\\ &\le -\frac{\gamma}{2}E_{cm2}^2-b\left(\frac{k}{2}+\alpha\right)E_{cm1}^2-|E_{cm2}|\left(\frac{1}{2}\gamma|E_{cm2}|-2\right)\\ &\quad -b|E_{cm1}|\left(\frac{1}{2}k|E_{cm1}|-2\right).\end{aligned} \tag{59}$$

Thus, as $|E_{cm2}| \ge 4/\gamma$ and $|E_{cm1}| \ge 4/k$, we have

$$\dot{V} \le -\frac{\gamma}{2}E_{cm2}^2-\frac{\gamma(k+2\alpha)}{4}E_{cm1}^2. \tag{60}$$

Let $\mu = \max\{4/k,4/\gamma\}$. From Theorem 4.18 in Khalil (2002), we conclude that the solutions of the averaged systems (56) are globally uniformly ultimately bounded. We denote a matrix P by

$$P = \begin{bmatrix}\frac{1}{2} & \frac{b}{2}\\ \frac{b}{2} & \frac{a^2}{2}\end{bmatrix}. \tag{61}$$

The ultimate bound of $(\|E_{cm1},E_{cm2}\|)$ is given by (Khalil, 2002, Section 4.8)

$$\sqrt{\frac{\lambda_{\max}(P)\mu^2}{\lambda_{\min}(P)}}. \tag{62}$$

The above result is summarized in the following theorem.

Theorem 2 (*Vibrational tracking control*). *The feedback vibrational controller* (35) *solves the tracking control problem defined in Section* 2.3.

Proof. Applying direct separation of the motion (Blekhman, 2000), we obtained the approximation system (52) for the "slow" dynamics of the closed-loop system (37) considering the effect of the fast vibration. We also showed that the approximate average system (52) is ultimately bounded by (62). The solution to the original system (37), in the form of (40), can be approximated by the solution of (52) with the error up to the order of $\varepsilon = 1/\omega$. Therefore, the tracking error, e, as defined in (36), is bounded, which in turn implies that z_{cm} tracks the reference position V_0t. □

Remark 3. Since z_{cm} tracks V_0t, the friction force defined in (7) is reduced in the closed-loop system. Also, the tracking control is a global result and applies to any initial conditions as no linearization is involved.

Theorem 2 achieves our main objective as to reduce friction force by vibration. However, even if the center of the mass system is stable, the single particle system could be unstable (for example, oscillating). Although individual particles do not need to be stable for friction to disappear, we are now interested in the effect of vibration on the single particle system. For this purpose, we discuss stability property of the single particle dynamics (53) in the next subsection.

4.2. Single particle dynamics in the closed-loop system

The stability of (53) is discussed in this subsection. Comparing it to the open-loop error system (11), we can see that in the closed-loop approximation system (53), the constant offset term $(-\gamma V_0)$ is canceled out, and an additional vibration term $(\sin V_0t)$ is added. It is easy to see that the equilibrium points of (53) are at $(E_{i1},E_{i2})=(0,0)$ for $i=1,\ldots,N$. Linearizing (53) around the equilibrium, we obtain

$$\dot{E}_{i1}=E_{i2},$$

$$\dot{E}_{i2}=-\cos(V_0t)\cdot E_{i1}-\gamma E_{i2}-\frac{(\alpha+k)}{N}\sum_{j=1}^{N}E_{j1}+\kappa(E_{i+1,1}-2E_{i1}+E_{i-1,1}). \tag{63}$$

Following the same procedure as presented in Section 3.2, we have the result summarized in the following theorem:

Theorem 3 (*Single particle stability in closed-loop system*). *If the system parameters, α,κ, V_0, and the control parameter k, satisfy the following conditions*:

$$\alpha+k>\frac{V_0}{\gamma}+1,\quad \kappa>\frac{1}{\mu_{N-1}}+\frac{V_0}{\gamma\mu_{N-1}}, \tag{64}$$

where μ_{N-1} is the second smallest eigenvalue of $(-Q)$ as defined in (17), *the system* (53) *is locally asymptotically stable around the equilibrium* $(E_{i1},E_{i2})=(0,0)$.

The proof of the theorem follows the same procedure as in the proof of Propositions 1 and 2 and is omitted here.

Remark 4. The condition (64) is less strict than (33) on the system parameter α. We can choose a relatively bigger control parameter k so that a small α ensures the asymptotical stability of single particles in the closed-loop system. Also, single particle position trajectories in the open-loop system is at the best ultimately bounded around $\gamma V_0/\alpha$, while they can be asymptotically stable in the closed-loop system.

5. Simulation results

Numerical simulations are performed on arrays of different sizes $(3\le N\le 256)$ using MATLAB. Simulation results are shown for the system parameters: $N=32$, $\gamma=0.1$, $\kappa=0.26$, $\alpha=1$, and $V_0=0.5$. Random initial conditions are chosen.

We first compare the center of the mass position and friction force between the open-loop system and the closed-loop system. In Fig. 3, we show the error position of the center of the mass of the particles. We can see that the center of the mass does not track the desired position signal V_0t well as the position error oscillates. Accordingly, the friction force, as defined in (7), is shown in Fig. 4, whose magnitude is around a non-zero constant. In comparison, for the closed-loop system with the feedback

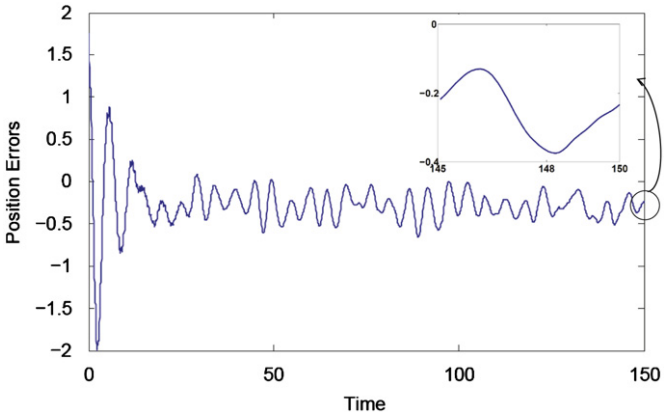

Fig. 3. Time history of the error position of the center of the mass in the open-loop system (11). Inset magnifies the response after $t=145$. The system parameters are $N=32$, $\gamma=0.1$, $\kappa=0.26$, $\alpha=1$, and $V_0=0.5$.

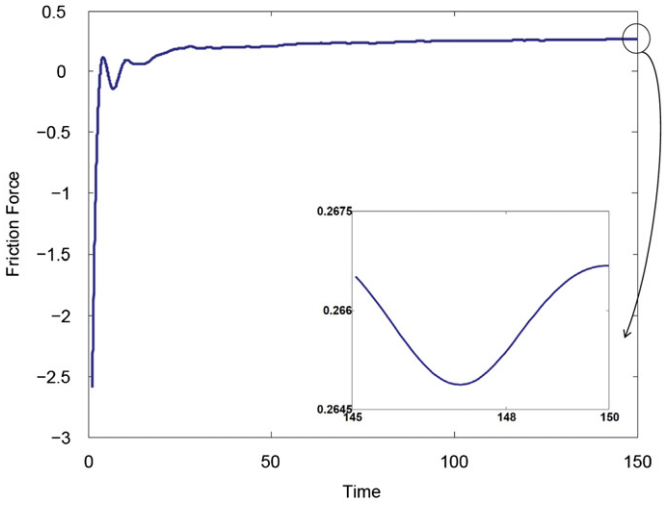

Fig. 4. Friction force of the open-loop system. Inset magnifies the response after $t=145$. The system parameters are the same as used in Fig. 3.

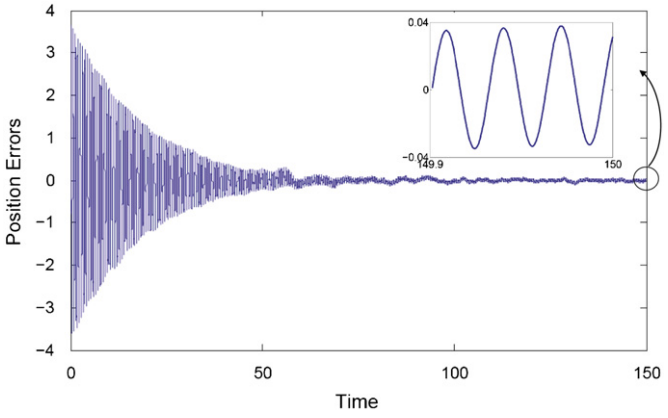

Fig. 5. Time history of the error position of the center of the mass in the closed-loop system under vibration control (35). Inset magnifies the response after $t=149.9$. The system parameters are the same as used in Fig. 3, and the control parameters are $k=30$, $c=50$, $\omega=200$.

vibration control (35), Fig. 5 shows the error position of the center of the mass in the closed-loop system, that is, the error state e as defined in (36). It demonstrates a good tracking control result. The corresponding friction force is shown in Fig. 6, which is

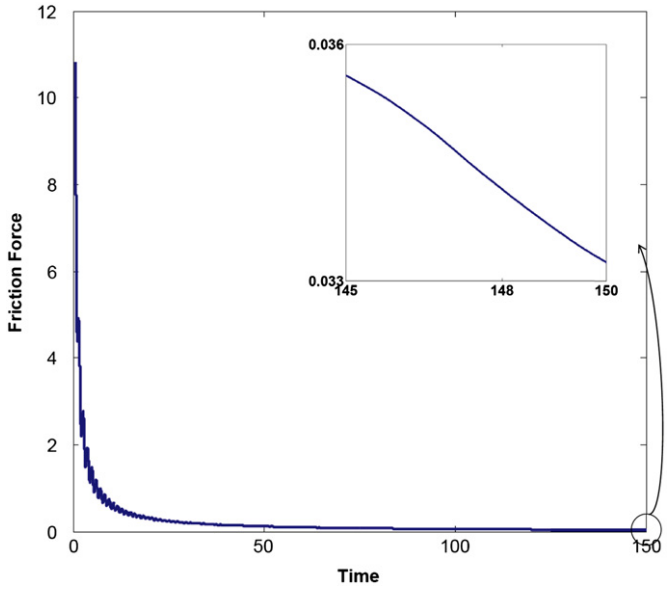

Fig. 6. Friction force of the closed-loop system. Inset magnifies the response after $t=145$. The parameters are the same as used in Fig. 5.

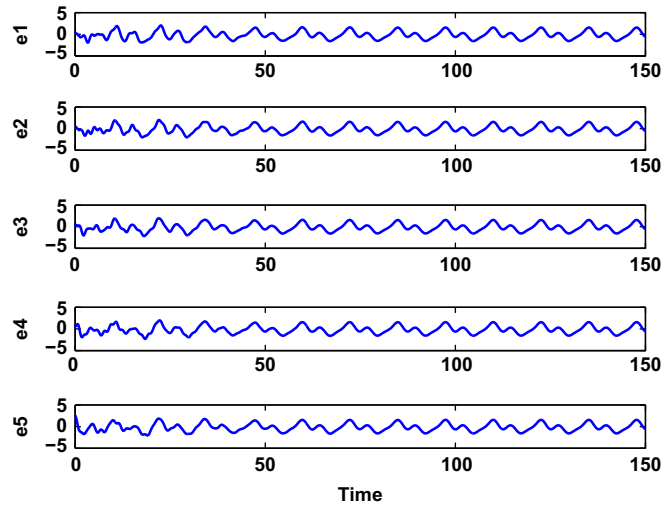

Fig. 7. Time history of the error positions of the individual particles in the open-loop system (11). The parameters are $N=5$, $\gamma=0.1$, $\kappa=5.3$, $\alpha=1$, and $V_0=0.5$.

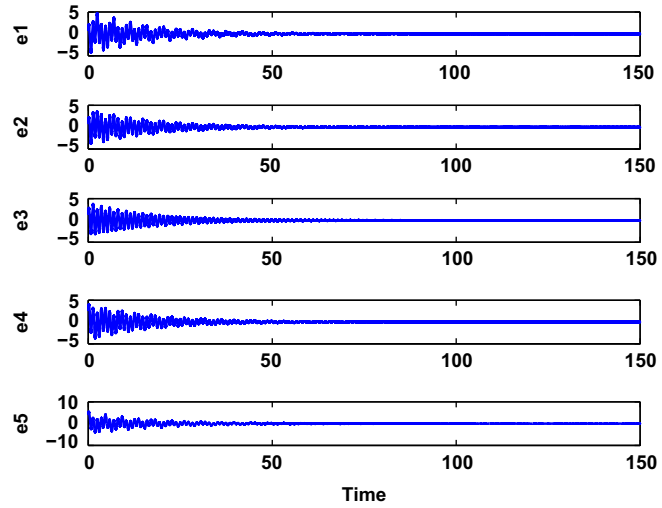

Fig. 8. Time history of the error positions of the individual particles in the closed-loop system. The system parameters are the same as used in Fig. 7, and the control parameters are $k=30$, $c=50$, $\omega=200$.

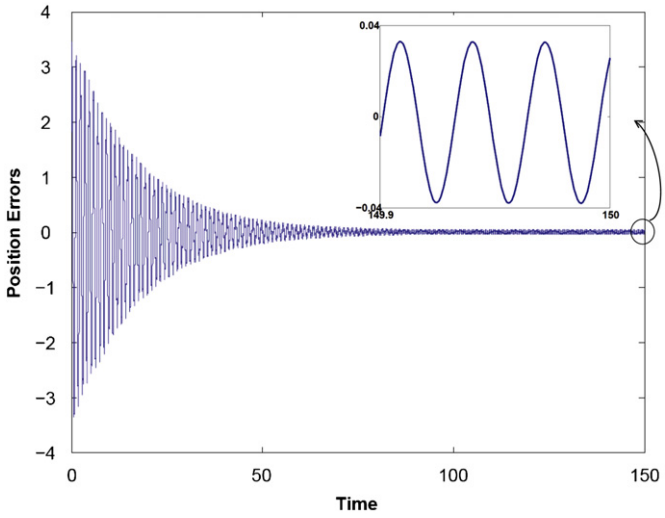

Fig. 9. Time history of the difference of the position variables between the closed-loop system (37) and its approximation system (52). Inset magnifies the response after $t=149.9$. The parameters are the same as used in Fig. 8.

very close to zero. The control parameters are chosen to be $k=30$, $c=50$, and the vibration frequency $\omega=200$.

We then compare the single particle trajectories in the open-loop and closed-loop systems. For this purpose, we change the system parameters $N=5,\kappa=5.3$, and keep all other system and control parameters unchanged. The open-loop performance, that is, the state e_{i1}, $i=1,\ldots,5$ in (11), is demonstrated in Fig. 7, which shows an oscillatory performance. Under the feedback vibration control law (35), the single particle trajectories converge in the closed-loop system as shown in Fig. 8.

In order to show how well the approximation system (52) matches the original closed-loop system (37), we plot the difference of the position variables between the two systems in Fig. 9, that is, $z_{cm1}-Z_{cm1}\stackrel{def}{=}(1/N)\sum_{i=1}^{N}z_i-(1/N)\sum_{i=1}^{N}Z_i$, where z_i and Z_i are the states of (37) and (52), respectively. We can see that the difference is close to zero as time elapses.

In the designed vibration control (35), the vibrational frequency, ω, is a high frequency constant chosen by the designer. In practice, the vibrational frequency is constrained by the device limitation and cannot be too high. To show the frequency dependent behavior of the friction force, we show numerical results in Table 1, where we show the value of F_{fric} at $t=150$ for the same initial condition randomly chosen. We can see that the differences between the friction forces at different frequencies are very small.

Note that in the above figures, the variables have no units as the simulations were performed based on the dimensionless model (3). Unit conversion of the vibration control is given in Appendix B, where units are given for the original variables in the model (1).

6. Conclusions

This paper discussed feedback vibration control to reduce friction force for an FFM sliding system. A dynamic model of the FFM system was first presented imitating the FFM tip as a 1D array of particles moving on a rigid substrate. The open-loop stability was studied, and it is revealed that both of the center of

Table 1
Frequency dependence of friction force.

Frequency ω	100	200	300	400	500	800
Friction force F_{fric}	0.0057	0.0056	0.0080	0.0078	0.0067	0.0073

the mass and the individual particles are ultimately bounded under severe system conditions. Then, a vibration control scheme was proposed so that high frequency vibration is applied to the substrate of the sliding system, and feedback vibration control was designed to reduce the tracking error of the closed-loop system, thus to reduce friction. With the help of direct separation of motion in vibrational mechanics (Blekhman, 2000), the tracking control objective was achieved, and relaxed conditions on the system parameters were obtained for single particles to be asymptotically stable. Numerical simulations using Matlab showed that the friction force under vibration control is reduced to almost zero. The proposed method may be applied to MEMS applications where superlubricity or extra-low friction are required. Future work includes experimental tests of the developed control, and quantitative comparisons with experimental results.

Acknowledgments

The work was partially supported by the National Science Foundation under Grants CMMI#0825613 and EFRI#1024660. Oak Ridge National Laboratory is managed by UT-Battelle, LLC for the U.S. Department of Energy under Contract DE-AC05-00OR22725.

Appendix A. Normalization of the sliding model (1)

In the following, we provide the normalization procedure from the original sliding system equation (1) to the dimensionless model (3).

Re-write (1)

$$m\ddot{\phi}_i+\gamma'\dot{\phi}_i+\frac{\partial U}{\partial \phi_i}=\alpha'(V_0't-\phi_{cm})+F_i(\phi_i,\phi_j). \tag{A.1}$$

Let the substrate potential be

$$U=\frac{1}{2}W\sum_{i=1}^{N}\left(1-\cos\left(\frac{2\pi\phi_i}{a}\right)\right), \tag{A.2}$$

where W is the energy constant in Joule, a is the surface periodicity in Meter. We get

$$\frac{\partial U_s}{\partial \phi_i}=\frac{\pi W}{a}\sin\left(\frac{2\pi\phi_i}{a}\right). \tag{A.3}$$

Let the inter-particle potential be

$$U_{int}=\frac{1}{2}K\sum_{i=1}^{N-1}(\phi_{i+1}-\phi_i-b)^2, \tag{A.4}$$

where b is the equilibrium inter-atomic distance, and K is the coupling coefficient. We get the inter-particle force

$$F_i(\phi_i,\phi_j)=\frac{\partial U_{int}}{\partial \phi_i}=K(\phi_{i+1}-2\phi_i+\phi_{i-1}). \tag{A.5}$$

Eq. (A.1) turns to

$$m\ddot{\phi}_i+\gamma'\dot{\phi}_i+\frac{\pi W}{a}\sin\left(\frac{2\pi\phi_i}{a}\right)=\alpha'(V_0't-\phi_{cm})+K(\phi_{i+1}-2\phi_i+\phi_{i-1}). \tag{A.6}$$

Define $z_i=2\pi\phi_i/a$, and divide both sides of the above equation by $\pi W/a$. We obtain

$$\frac{ma^2}{2W\pi^2}\ddot{z}_i+\frac{\gamma'a^2}{2W\pi^2}\dot{z}_i+\sin(z_i)=\frac{a}{\pi W}\alpha'(V_0't-z_{cm})+\frac{Ka^2}{2W\pi^2}(z_{i+1}-2z_i+z_{i-1}). \tag{A.7}$$

Define

$$\omega_0^2=\frac{2W\pi^2}{ma^2}. \tag{A.8}$$

Then define the dimensionless time $\tau=\omega_0 t$. After simplification, we have

$$\frac{d^2z_i}{d\tau^2}+\frac{\gamma'a^2}{2W\pi^2}\omega_0\frac{dz_i}{d\tau}+\sin(z_i)=\frac{a^2}{2\pi^2W}\alpha'\left(\frac{2\pi}{a\omega_0}V_0'\tau-z_{cm}\right)+\frac{Ka^2}{2W\pi^2}(z_{i+1}-2z_i+z_{i-1}). \tag{A.9}$$

Define

$$\gamma=\frac{\gamma'a^2}{2W\pi^2}\omega_0=\frac{\gamma'a^2}{2W\pi^2}\sqrt{\frac{ma^2}{2W\pi^2}}, \tag{A.10}$$

$$\kappa=\frac{Ka^2}{2W\pi^2}, \tag{A.11}$$

$$\alpha=\frac{a^2}{2\pi^2W}\alpha', \tag{A.12}$$

$$V_0=\frac{2\pi}{a\omega_0}V_0'. \tag{A.13}$$

We obtain the dimensionless equation (where the derivatives are with respect to the dimensionless time τ),

$$\ddot{z}_i+\gamma\dot{z}_i+\sin(z_i)=\alpha(V_0t-z_{cm})+\kappa(z_{i+1}-2z_i+z_{i-1}). \tag{A.14}$$

This is Eq. (3).

Appendix B. Unit conversion of vibration control

If we add a term of the vibrational external force, f'_{vi}, in the right hand side of Eq. (A.1), following the same normalization procedure as described in Appendix A, we obtain

$$f_{vi}=\frac{a}{\pi W}f'_{vi}. \tag{B.1}$$

Since the vibration control (35) is designed based on the dimensionless model (A.14), that is,

$$f_{vi}=\sin(\omega\tau)\cdot\left(\omega\sqrt{2ke^2-4\gamma V_0e-4\sin(V_0\tau)e+c}\right), \tag{B.2}$$

the actual friction force applied to the sliding system is

$$f'_{vi}=\frac{\pi W}{a}f_{vi}, \tag{B.3}$$

$$f'_{vi}=\frac{\pi W}{a}\left(\omega\sqrt{2ke^2-4\gamma V_0e-4\sin(V_0t)e+c}\right)\sin(\omega\omega_0t), \tag{B.4}$$

$$f'_{vi}\stackrel{def}{=}A'\sin(\omega't). \tag{B.5}$$

Consider the parameters in the original system (A.1) of the following values:

$$m = 0.12 \text{ nkg}, \quad a = 3 \text{ nm}, \quad W = 1 \times 10^{-10} \text{ nJ}. \tag{B.6}$$

Assume the AFM scan size is $l = 10$ μm, using the parameter of the simulation, $V_0 = 0.5$, we get $V_0' = 9.5$ μm/s. So the AFM scan frequency is $f = 1/T = V_0'/l = 0.95$ Hz.

Using the control parameters of the simulations, that is,

$$\omega = 200, \quad c = 50, \quad k = 30, \tag{B.7}$$

we have the actual vibration frequency and amplitude:

$$\omega' = \omega\omega_0 = 200 \times 4 \times 10^4 = 8 \text{ MHz}, \tag{B.8}$$

$$A' = \frac{\pi W}{a}\omega\sqrt{c} = 0.148 \text{ μm}. \tag{B.9}$$

Note that we take $e \approx 0$ around the steady state in calculating A'.

As the control result seen from the simulations (Figs. 4 and 6), the non-dimensional friction force is reduced from around 0.26 to 0.03. After the unit conversion ($F_{fric}' = F_{fric} * \pi W/a$), the friction force is reduced from 2.7×10^{-2} nN to 3×10^{-3} nN by using the designed vibration control.

References

Abel, D. G., Krylov, S. Y., & Frenken, J. W. M. (2007). Evidence for contact delocalization in atomic scale friction. *Physical Review Letters*, *99*(16), 166102.

Bellman, R. E., Bentsman, J., & Meerkov, S. M. (1986). Vibrational control of nonlinear systems: Vibrational stability. *IEEE Transactions on Automatic Control*, *31*(8), 710–716.

Bentsman, J. (1987). Vibrational control of a class of nonlinear systems by nonlinear multiplicative vibrations. *IEEE Transactions on Automatic Control*, *32*(8), 711–716.

Blekhman, I. I. (2000). *Vibrational mechanics: Nonlinear dynamic effects, general approach, applications*. World Scientific.

Bogoliubov, N. N., & Mitropolsky, Y. A. (1961). *Asymptotic methods in the theory of nonlinear oscillations*. New York: Gordon and Breach.

Braiman, Y., Barhen, J., & Protopopescu, V. (2003). Control of friction at the nanoscale. *Physical Review Letters*, *90*(9).

Braiman, Y., Family, F., & Hentschel, H. G. E. (1997). Nonlinear friction in the periodic stick-slip motion of coupled oscillators. *Physical Review B*, *55*(8), 5491–5504.

Braun, O., & Naumovets, A. (2006). Nanotribology: Microscopic mechanisms of friction. *Surface Science Reports*, *60*, 79–158.

Braun, O. M., & Ferrando, R. (2002). Role of long jumps in surface diffusion. *Physical Review E*, *65*(6), 061107.

Bullo, F. (2002). Averaging and vibrational control of mechanical systems. *SIAM Journal on Control and Optimization*, *41*(2), 542–562.

Dudko, O., Filippov, A., Klafter, J., & Urbakh, M. (2002). Chemical control of friction: Mixed lubricant monolayers. *Tribology Letters*, *12*(4), 217–227.

Elmer, F. J. (1997). Nonlinear dynamics of dry friction. *Journal of Physics A*, *30*(17), 6057–6063.

Gnecco, E., Bennewitz, R., Gyalog, T., & Meyer, E. (2001). Friction experiments on the nanometer scale. *Journal of Physics: Condensed Matter*, *13*, R619–R642.

Guo, Y., & Qu, Z. (2008). Control of frictional dynamics of a one-dimensional particle array. *Automatica*, *44*, 2560–2569.

Guo, Y., Qu, Z., Braiman, Y., Zhang, Z., & Barhen, J. (2008). Nanotribology and nanoscale friction: Smooth sliding through feedback control. *IEEE Control Systems Magazine*, *28*(6), 92–100.

Helman, J. S., Baltensperger, W., & Holyst, J. A. (1994). Simple-model for dry friction. *Physical Review B*, *49*(6), 3831–3838.

Heuberger, M., Drummond, C., & Israelachvili, J. N. (1998). Coupling of normal and transverse motions during frictional sliding. *Journal of Physics and Chemistry B*, *102*, 5038–5041.

Hinrichs, N. (1997). Reibungsschwingungen mit selbst-und fremderregung: Experiment, modellierung und berechnung. *Fortschritt-Berichte*, *240*, 124.

Jeon, S., Thundat, T., & Braiman, Y. (2006). Effect of normal vibration on friction in the atomic force microscopy experiment. *Applied Physics Letters*, *88*(1), 214102.1–214102.3.

Jeon, S., Thundat, T., & Braiman, Y. (2007). Frictional dynamics at the atomic scale in presence of small oscillations of the sliding surfaces. In A. Erdemir, & J. M. Martin (Eds.), *Superlubricity* (pp. 119–130). Elsevier.

Khalil, H. (2002). *Nonlinear systems* (3rd ed.). Prentice-Hall.

Klafter, J., & Urbakh, M. (2007). The basics of nanoscale friction and ways to control it. In E. Gnecco, & E. Meyer (Eds.), *Fundamentals of friction and wear on the nanoscale* (pp. 143–158). Berlin, Heidelberg: Springer.

Krylov, S. Y., & Frenken, J. W. M. (2008). The crucial role of temperature in atomic scale friction. *Journal of Physics: Condensed Matter*, *20*(35), 354003.

Krylov, S. Y., & Frenken, J. W. M. (2009). Atomic-scale friction experiments reconsidered in the light of rapid contact dynamics. *Physical Review B*, *80*(23), 235435.

Meerkov, S. M. (1980). Principle of vibration control: Theory and applications. *IEEE Transactions on Automatic Control*, *25*, 755–762.

Miret-Artés, S., & Pollak, E. (2005). The dynamics of activated surface diffusion. *Journal of Physics: Condensed Matter*, *17*, S4133.

Miyoshi, T., Masuia, Y., & Terashimaa, K. (2007). Development of high-stiffness touch sensor and its application to measuring instruments. *Control Engineering Practice*, *15*(7), 851–862.

Nakamura, J., Wakunami, S., & Natori, A. (2005). Double-slip mechanism in atomic-scale friction: Tomlinson model at finite temperatures. *Physical Review B*, *72*(23), 235415.

Persson, B. N. J. (1997). Theory of friction: Friction dynamics for boundary lubricated surfaces. *Physical Review B*, *55*(12), 8004–8012.

Persson, B. N. J. (2000). *Sliding friction* (2nd ed.). Springer.

Persson, B. N. J., & Nitzan, A. (1996). Linear sliding friction: On the origin of the microscopic friction for Xe on silver. *Surface Science*, *367*(3), 261–275.

Pervozvanski, A. A., & de Wit, C. C. (2002). Asymptotic analysis of the dither effect in systems with friction. *Automatica*, *38*, 105–113.

Qu, Z. (1998). *Robust control of nonlinear uncertain systems. Wiley sciences in nonlinear science*. John Wiley & Sons.

Rifai, O. M. E., & Youcef-Toumia, K. (2007). On automating atomic force microscopes: An adaptive control approach. *Control Engineering Practice*, *15*(3), 349–361.

Ruan, J. A., & Bhushan, B. (1994). Atomic-scale friction measurements using friction force microscopy: Part I—General principles and new measurement techniques. *Transactions of the ASME*, *116*(April), 378–388.

Shapiro, B., & Zinn, B. T. (1997). High-frequency nonlinear vibrational control. *IEEE Transactions on Automatic Control*, *42*(1), 83–90.

Smith, E. D., Robbins, M. O., & Cieplak, M. (1996). Friction on adsorbed monolayers. *Physical Review B*, *54*(11), 8252–8260.

Socoliuc, A., Bennewitz, R., Gnecco, E., & Meyer, E. (2004). Transition from stick-slip to continuous sliding in atomic friction: Entering a new regime of ultralow friction. *Physical Review Letters*, *92*, 134301.

Socoliuc, A., Gnecco, E., Maier, S., Pfeiffer, O., Baratoff, A., Bennewitz, R., & Meyer, E. (2006). Atomic-scale control of friction by actuation of nanometer-sized contacts. *Science*, *313*, 207–210.

Sokoloff, J. B. (1995). Theory of the contribution to sliding friction from electronic excitations in the microbalance experiment. *Physical Review B*, *52*(7), 5318–5322.

Tshiprut, Z., Filippov, A. E., & Urbakh, M. (2005). Tuning diffusion and friction in microscopic contacts by mechanical excitations. *Physical Review Letters*, *95*, 016101.

Urbakh, M., Klafter, J., Gourdon, D., & Israelachvili, J. (2004). The nonlinear nature of friction. *Nature*, *430*, 525–528.

Vanossi, A., & Braun, O. M. (2007). Driven dynamics of simplified tribological models. *Journal of Physics: Condensed Matter*, *19*, 305017-1–305017-21.

Weiss, M., & Elmer, F. J. (1996). Dry friction in the Frenkel–Kontorova–Tomlinson model: Static properties. *Physical Review B*, *53*(11), 7539–7549.

Wu, Y., & Zou, Q. (2009). An iterative-based feedforward-feedback control approach to high-speed atomic force microscope imaging. *Journal of Dynamic Systems, Measurement and Control, Transactions of the ASME*, *131*(6), 1–9.

Zaloj, V., Urbakh, M., & Klafter, J. (1999). Modifying friction by manipulating normal response to lateral motion. *Physical Review Letters*, *82*, 4823–4826.

Zames, G., & Shneydor, N. A. (1977). Structural stabilization and quenching by dither in nonlinear systems. *IEEE Transactions on Automatic Control*, *22*(3), 352–361.

Zworner, O., Holscher, H., Schswarz, U. D., & Wiesendanger, R. (1998). The velocity dependence of frictional forces in point-contact friction. *Applied Physics A*, *66*, S263–S267.